

Centralized Learning of the Distributed Downlink Channel Estimators in FDD Systems using Uplink Data

Benedikt Fesl, Nurettin Turan, Michael Koller, Michael Joham, and Wolfgang Utschick
Professur für Methoden der Signalverarbeitung, Technische Universität München, 80290 Munich, Germany
Email: {benedikt.fesl, nurettin.turan, michael.koller, joham, utschick}@tum.de

Abstract—In this work, we propose a convolutional neural network (CNN) based low-complexity approach for downlink (DL) channel estimation (CE) in frequency division duplex (FDD) systems. In contrast to existing work, we use training data which solely stems from the uplink (UL) domain. This allows to learn the CNN centralized at the base station (BS). After training, the network parameters are offloaded to mobile terminals (MTs) within the coverage area of the BS. The MTs can then obtain channel state information (CSI) of the MIMO channels with the low-complexity CNN estimator. This circumvents the necessity of an infeasible amount of feedback, i.e., acquisition of training data at the user, and the offline training phase at each MT. Numerical results show that the CNN which is trained solely based on UL data performs equally well as the network trained based on DL data. Furthermore, the approach is able to outperform state-of-the-art CE algorithms.

Index Terms—Channel estimation, massive MIMO, machine learning, neural networks, FDD systems.

I. INTRODUCTION

Massive MIMO is a key technology to greatly enhance the wireless communication capacity and throughput due to the increased degrees of freedom [1]. To exploit the spatial multiplexing and array gains to their full extent, accurate knowledge of the CSI is important. A variety of approaches for CE concentrate on time division duplex (TDD) mode, where channel reciprocity is present and the UL CSI can be exploited for the DL as well. However, due to the limited coherence time and the calibration error of radio frequency chains, the estimated CSI at the BS may not be accurate for the DL [2]. Furthermore, in FDD mode, more efficient communication with lower latency, improved coverage, and reduced interference can be realized [3]. This makes FDD an attractive option for future generations of mobile communication.

In FDD systems, channel reciprocity does not hold and DL CE has to be performed at the user who then sends some information regarding the DL CSI via a feedback link to the BS. Due to the large dimensions, this is especially challenging in massive MIMO because of an increasing pilot overhead with increasing number of BS antennas, a significantly large feedback size, and limited computational power at the user due to energy efficiency constraints. Many approaches for DL CE in FDD systems take structural information like sparsity or low-rank models into account in order to utilize compressive

sensing (CS)-based reconstruction techniques [4] – [7]. However, in many of those works, the feedback overhead is very high and would be infeasible in real systems. Furthermore, the CS-based approaches do not account for complex statistical correlations that are hard to model nor do they consider structure beyond sparse or low-rank patterns.

Very recently, deep learning based approaches have been used for pilot design, channel estimation, compression, feedback design, or a combination of these topics, e.g., [8] – [10]. By training the networks with channels from the corresponding scenario, it is possible to learn complex underlying statistical correlations and structures. Consequently, these approaches are generally able to outperform the CS-based approaches. However, in none of these works the following crucial aspects are discussed:

- Generation of a training dataset in operation mode at the MT with measured channels; alternatively, the sharing of a dataset which is stored at the BS with the MT which causes excessive overhead.
- Storage of a training dataset at the MT.
- Computational complexity and power consumption of the offline training, especially when users move from one cell to another with different environmental structures and a different BS location where re-training may be necessary.

A. Proposed Learning Strategy

In order to prevent these described problems of learning-based approaches, we propose a learning strategy where the network is trained solely based on UL channel data directly at the BS by emulating the DL system with transposed UL channels. Only the network parameters, i.e., the weights and biases of the neural network, have to be shared with the user in an initialization stage, e.g., when a MT enters the coverage area of the BS. Fig. 1 summarizes the procedure:

- 1) Construction of a training dataset \mathcal{H}^{UL} from UL channels at the BS.
- 2) Transposition of the channels in \mathcal{H}^{UL} and emulation of the DL system to train CNN at the BS.
- 3) Offloading of the CNN parameters to the MTs.
- 4) CE at the MT with low-complexity CNN.

A further possibility is a signaling approach where MTs in a certain sector of the coverage area can be updated with adjusted network parameters that are trained offline beforehand,

This work was funded by Huawei Sweden Technologies AB, Lund.

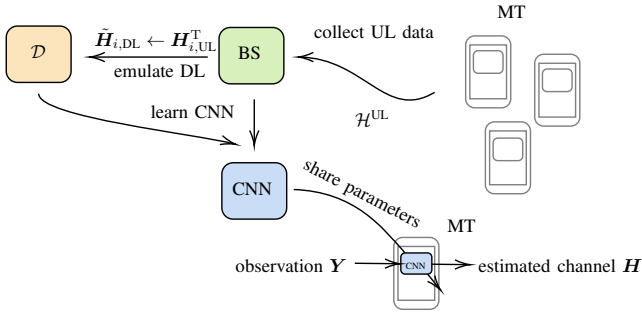


Fig. 1: The proposed approach of learning the CNN CE at the BS, which is then subsequently offloaded to the MT.

e.g., if a MT changes from a line of sight (LOS) to a non-line of sight (NLOS) channel, for example, by moving inside or behind a building, and therefore has different channel statistics. In other words, because the network is trained centralized at the BS, the opportunity to provide MTs in different sectors of the coverage area with different network parameters is given, due to available long-term statistics which can be inferred from the UL domain.

The motivation for this procedure stems from a recently developed UL-DL conjecture, stating that the distributions of UL and DL channels are very similar, although the instantaneous channels between UL and DL are highly different [11], [12]. This follows from the fact that a frequency shift, which is present between UL and DL in FDD systems, can be alternatively described by a change in the path length, or by a change of the antenna positioning, at least for narrowband signals. Consequently, for a certain propagation scenario it can be expected that there exist different pairs of antenna positions and carrier frequencies with identical CSI [11]. In [13], this UL-DL conjecture is exploited for adaptive codebook construction and feedback generation.

In general, this learning strategy is applicable to any learning-based approach which is trained on channel data. In this work, we apply it to the recently proposed low-complexity CNN estimator for MIMO channels [14] which is based on the original approach from [15] and learns a model-based CNN architecture, motivated by the conditional mean estimator. Numerical results demonstrate that the CNN estimator trained on UL data performs equally well in terms of mean squared error (MSE) as the CNN estimator trained on DL data. Moreover, the proposed approach is able to outperform state-of-the-art CE approaches in different scenarios.

Notation: The transpose and conjugate-transpose of a vector \mathbf{x} are denoted by \mathbf{x}^T and \mathbf{x}^H . The $n \times n$ identity matrix and the $n \times 1$ all-ones vector are denoted by \mathbf{I}_n and $\mathbf{1}_n$, respectively. The column-wise vectorization and the trace of a matrix \mathbf{X} are denoted by $\text{vec}(\mathbf{X})$ and $\text{tr}(\mathbf{X})$ and the Kronecker product by \otimes . A diagonal matrix with diagonal \mathbf{x} is given by $\text{diag}(\mathbf{x})$.

II. SYSTEM MODEL

We consider a DL scenario, where N_P pilot signals are transmitted. At the BS and the MT uniform linear arrays (ULAs) with N_{tx} and N_{rx} antennas are deployed, respectively.

The channel is assumed to be frequency-flat with block-fading such that we get independent observations in each coherence interval. We investigate a single-snapshot scenario, i.e., the coherence interval of the covariance matrix and of the channel is identical. The received signal is $\mathbf{Y} = \mathbf{H}\mathbf{X}' + \mathbf{Z}$ with the channel matrix $\mathbf{H} \in \mathbb{C}^{N_{\text{rx}} \times N_{\text{tx}}}$ and the pilot matrix $\mathbf{X}' \in \mathbb{C}^{N_{\text{tx}} \times N_P}$. After vectorization we get

$$\mathbf{y} = \mathbf{X}\mathbf{h} + \mathbf{z} \in \mathbb{C}^{N_{\text{rx}}N_P}, \quad (1)$$

with $\mathbf{X} = \mathbf{X}'^T \otimes \mathbf{I}_{N_{\text{rx}}}$ and $\mathbf{h} = \text{vec}(\mathbf{H}) \in \mathbb{C}^{N_{\text{tx}}N_{\text{rx}}}$. Note that we use the channel matrix \mathbf{H} and its vectorized expression \mathbf{h} interchangeably in the following for the ease of notation. We choose a scaled discrete Fourier transform (DFT) matrix $\mathbf{X}' = \frac{1}{\sqrt{N_{\text{tx}}}}\mathbf{F}$ as pilot matrix, where \mathbf{F} is the DFT matrix [16]. The noise vector is assumed to be distributed as $\mathbf{z} \sim \mathcal{N}_{\mathbb{C}}(\mathbf{0}, \sigma^2\mathbf{I}_{N_{\text{rx}}N_P})$.

III. CHANNEL MODEL AND DATA GENERATION

We consider an FDD system and assume a frequency gap of 200 MHz between UL and DL. Version 2.2 of the QuaDRiGa channel simulator [17], [18] is used to generate CSI for the UL and DL scenarios. We simulate two urban macrocell (UMa) single carrier scenarios: one with $(N_{\text{tx}}, N_{\text{rx}}) = (8, 4)$ and one with $(N_{\text{tx}}, N_{\text{rx}}) = (64, 4)$. In both cases, the UL carrier frequency is 2.53 GHz and the DL carrier frequency is 2.73 GHz. The BS is equipped with a ULA with “3GPP-3D” antennas, and the MT consists of a ULA assuming “omni-directional” antennas. The BS is placed at a height of 25 m and covers a sector of 120° , where the minimum distance of the MT location to the BS is 35 m and the maximum distance to the BS is 500 m. In 80% of the cases, the MT is located indoors at different floor levels, and in the case of outdoor locations the MT’s height is 1.5 m in accordance with [19]. Simulation results were also carried out for different center frequencies and for the urban microcell (UMi) scenario, but displayed qualitatively the same results and are therefore not shown here.

As outlined in [17], many parameters such as path-loss, delay, and angular spreads, path-powers for each subpath, and antenna patterns are different in the UL and DL domain. However, the following parameters are identical in the UL and DL domain: BS location and the MT locations, propagation cluster delays and angles for each multi-path component (MPC), and the spatial consistency of the large scale fading parameters. QuaDRiGa models MIMO channels as

$$\mathbf{H} = \sum_{\ell=1}^L \mathbf{G}_\ell e^{-2\pi j f_c \tau_\ell}, \quad (2)$$

where ℓ is the path number, and the number of MPCs L depends on whether there is LOS, NLOS, or outdoor-to-indoor (O2I) propagation: $L_{\text{LOS}} = 37$, $L_{\text{NLOS}} = 61$, or $L_{\text{O2I}} = 37$. The carrier frequency is denoted by f_c and the ℓ -th path delay by τ_ℓ . The MIMO coefficient matrix \mathbf{G}_ℓ consists of one complex entry for each antenna pair, which comprises the attenuation of a path, the antenna radiation pattern weighting, and the

polarization [20]. Each channel is normalized using its path gain as $\mathbf{H} = 10^{-0.05\text{PG}[\text{dB}]} \mathbf{H}_{\text{raw}}$ according to [18].

We generate datasets with 31×10^3 channels for both the UL and DL of each scenario, where 1000 channels are used to calculate a global sample covariance matrix

$$\widehat{\mathbf{C}}_{\text{glob}} = \frac{1}{1000} \sum_{i=1}^{1000} \mathbf{h}_i \mathbf{h}_i^H, \quad (3)$$

for both UL and DL, respectively. The channels which are used for the calculation of the sample covariance matrix are not further used for training or evaluation. The training dataset contains 20×10^3 channels, whereas the performance of the different approaches are averaged over 10×10^3 channels in the test dataset. For each dataset of UL and DL, the channels are normalized, such that it holds: $E[||\mathbf{h}||^2] = N_{\text{tx}}N_{\text{rx}}$. Accordingly, we define the signal-to-noise ratio (SNR) as $\text{SNR} = E[||\mathbf{X}\mathbf{z}||_F^2]/E[||\mathbf{z}||_2^2] = 1/\sigma^2$. This leads to the following pairs of UL and DL datasets for the two considered scenarios:

$$(\mathcal{H}_{4 \times 8}^{\text{UL}}, \mathcal{H}_{4 \times 8}^{\text{DL}}) \text{ and } (\mathcal{H}_{4 \times 64}^{\text{UL}}, \mathcal{H}_{4 \times 64}^{\text{DL}}). \quad (4)$$

The UL channels have a dimension of 8×4 or 64×4 depending on the scenario. The sets $\mathcal{H}_{4 \times 8}^{\text{UL}}$ and $\mathcal{H}_{4 \times 64}^{\text{UL}}$ contain transposed versions of the respective channels, i.e., with dimensions 4×8 or 4×64 .

IV. REVISION OF THE CNN ESTIMATOR

In the following, we give a short revision of the CNN estimator from [14]. We assume that for a given variable δ , the channels are conditionally Gaussian distributed as $\mathbf{h}|\delta \sim \mathcal{CN}(\mathbf{0}, \mathbf{C}_\delta)$. The vector δ contains prior information such as angles of arrival or path gains and follows an unknown distribution $\delta \sim p(\delta)$. Assuming knowledge of the prior parameters δ , the conditional minimum mean squared error (MMSE) estimate of \mathbf{h} from \mathbf{y} would read as

$$E[\mathbf{h}|\mathbf{y}, \delta] = E[\mathbf{h}\mathbf{y}^H|\delta]E[\mathbf{y}\mathbf{y}^H|\delta]^{-1}\mathbf{y} \quad (5)$$

$$= \mathbf{C}_\delta \mathbf{X}^H (\mathbf{X} \mathbf{C}_\delta \mathbf{X}^H + \sigma^2 \mathbf{I}_{N_{\text{rx}}N_P})^{-1} \mathbf{y} = \mathbf{W}_\delta \mathbf{y}, \quad (6)$$

which depends linearly on the observations. However, as the parameters δ are unknown in general, the law of total expectation is used to compute [15]

$$\hat{\mathbf{h}} = E[\mathbf{h}|\mathbf{y}] = E[E[\mathbf{h}|\mathbf{y}, \delta]|\mathbf{y}] = E[\mathbf{W}_\delta \mathbf{y}|\mathbf{y}] = \widehat{\mathbf{W}}_\star(\mathbf{y})\mathbf{y}. \quad (7)$$

Thus, to obtain $\hat{\mathbf{h}}$, the conditional mean $\widehat{\mathbf{W}}_\star$ of the MMSE filter \mathbf{W}_δ has to be determined, which nonlinearly depends on \mathbf{y} .

Bayes' theorem is used to state the MMSE filter as [15]

$$\widehat{\mathbf{W}}_\star = \int p(\delta|\mathbf{y}) \mathbf{W}_\delta d\delta = \frac{\int p(\mathbf{y}|\delta) \mathbf{W}_\delta p(\delta) d\delta}{\int p(\mathbf{y}|\delta) p(\delta) d\delta}. \quad (8)$$

As shown in [14], due to the Gaussian assumption of \mathbf{y} given δ , the MMSE filter can be written as

$$\widehat{\mathbf{W}}(\widehat{\mathbf{C}}) = \frac{\int \exp(\text{tr}(\mathbf{X} \mathbf{W}_\delta \widehat{\mathbf{C}}) + \log |\mathbf{I} - \mathbf{X} \mathbf{W}_\delta|) \mathbf{W}_\delta p(\delta) d\delta}{\int \exp(\text{tr}(\mathbf{X} \mathbf{W}_\delta \widehat{\mathbf{C}}) + \log |\mathbf{I} - \mathbf{X} \mathbf{W}_\delta|) p(\delta) d\delta}, \quad (9)$$

with the scaled single-shot sample covariance matrix $\widehat{\mathbf{C}} = \frac{1}{\sigma^2} \mathbf{y}\mathbf{y}^H$ as input. The MMSE filter $\widehat{\mathbf{W}}_\star$ depends on the observations through $\widehat{\mathbf{C}}$ and is thus a nonlinear filter. For an arbitrary distribution $p(\delta)$, the MMSE filter in (9) is not computable. To overcome this problem, the prior distribution is assumed to be discrete and uniform on a grid $\{\delta_i : i = 1, \dots, P\}$ with $p(\delta_i) = 1/P$ for all $i = 1, \dots, P$, cf. [14]. With this assumption, the MMSE estimator is evaluated as

$$\widehat{\mathbf{W}}_{\text{GE}}(\widehat{\mathbf{C}}) = \frac{1/P \sum_{i=1}^P \exp(\text{tr}(\mathbf{X} \mathbf{W}_{\delta_i} \widehat{\mathbf{C}}) + b_i) \mathbf{W}_{\delta_i}}{1/P \sum_{i=1}^P \exp(\text{tr}(\mathbf{X} \mathbf{W}_{\delta_i} \widehat{\mathbf{C}}) + b_i)}, \quad (10)$$

with $b_i = \log |\mathbf{I} - \mathbf{X} \mathbf{W}_{\delta_i}|$. This approximates $\widehat{\mathbf{W}}(\widehat{\mathbf{C}})$, where the approximation error decreases with increasing P [15].

The complexity of the estimator can be reduced by exploiting common structure of the covariance matrices, i.e., it is assumed that the channel covariance matrix is a block-circulant matrix with circulant blocks, which only holds asymptotically for large-scale systems [14]. As such a matrix is decomposed by a two-dimensional DFT matrix \mathbf{Q} , i.e., $\mathbf{C}_\delta = \mathbf{Q}^H \text{diag}(\mathbf{c}_\delta) \mathbf{Q}$, the MMSE filter from (6) can be decomposed as $\mathbf{W}_\delta = \mathbf{Q}^H \text{diag}(\mathbf{w}_\delta) \mathbf{Q}$. With this assumption, the MMSE filter from (10) is approximately

$$\widehat{\mathbf{W}}(\hat{\mathbf{c}}) \approx \mathbf{Q}^H \text{diag}(\mathbf{w}(\hat{\mathbf{c}})) \mathbf{Q} \mathbf{X}^H, \quad (11)$$

with the definitions

$$\mathbf{w}(\hat{\mathbf{c}}) = \mathbf{A} \frac{\exp(\mathbf{A}^T \hat{\mathbf{c}} + \mathbf{b})}{\mathbf{1}_P^T \exp(\mathbf{A}^T \hat{\mathbf{c}} + \mathbf{b})}, \quad (12)$$

$$\mathbf{A} = [\mathbf{w}_{\delta_1}, \dots, \mathbf{w}_{\delta_P}] \in \mathbb{C}^{N_{\text{rx}} N_{\text{tx}} \times P}, \quad (13)$$

$$\hat{\mathbf{c}} = \sigma^{-2} |\mathbf{Q} \mathbf{X}^H \mathbf{y}|^2 \in \mathbb{C}^{N_{\text{rx}} N_{\text{tx}}}, \quad (14)$$

and $\mathbf{b} = [b_{\delta_1}, \dots, b_{\delta_P}]^T$ as shown in [14, Appendix C].

The complexity is further reduced by assuming \mathbf{A} to be a block-circulant matrix with circulant blocks, which is valid for specific scenarios, i.e., a single propagation cluster, cf. [14]. Following this assumption, there exists a \mathbf{w}_0 such that $\mathbf{A} = \mathbf{Q}^H \text{diag}(\mathbf{Q} \mathbf{w}_0) \mathbf{Q}$. This is equal to constructing \mathbf{A} by a two-dimensional circular convolution with \mathbf{w}_0 as convolution kernel and we can write $\mathbf{A} \mathbf{x} = \mathbf{w}_0 \star \mathbf{x}$. The estimator containing all three assumptions can then be written as

$$\widehat{\mathbf{W}}(\hat{\mathbf{c}}) = \mathbf{Q}^H \text{diag}(\mathbf{w}_0 \star \phi(\tilde{\mathbf{w}}_0 \star \hat{\mathbf{c}} + \mathbf{b})) \mathbf{Q} \mathbf{X}^H, \quad (15)$$

where ϕ is the softmax function and $\tilde{\mathbf{w}}_0$ contains the entries of \mathbf{w}_0 in reversed order.

These assumptions for the derivation may only rarely be fulfilled in real scenarios. Therefore, the estimator from (15) is interpreted as a CNN with two two-dimensional convolution layers, which implements a function from the set

$$\mathcal{W}_{\text{CNN}} = \{\mathbf{x} \mapsto \mathbf{a}^{(2)} \star \psi(\mathbf{a}^{(1)} \star \mathbf{x} + \mathbf{b}^{(1)}) + \mathbf{b}^{(2)}\}, \quad (16)$$

where $\mathbf{a}^{(l)}, \mathbf{b}^{(l)} \in \mathbb{R}^{N_{\text{rx}} N_{\text{tx}}}$, $l = 1, 2$ are the parameters which are learned during training from samples $(\mathbf{y}_i, \mathbf{h}_i)$. Although the softmax function ϕ is identified as the activation in (15), the activation is relaxed to be a different function ψ , e.g., the

well-known rectified linear unit (ReLU). The optimal CNN estimator is the function which minimizes the MSE, i.e.,

$$\hat{\mathbf{w}}_{\text{CNN}} = \arg \min_{\hat{\mathbf{w}}(\cdot) \in \mathcal{W}_{\text{CNN}}} \mathbb{E}[|\|\mathbf{h} - \mathbf{Q}^{\text{H}} \text{diag}(\hat{\mathbf{w}}(\hat{\mathbf{c}})) \mathbf{Q} \mathbf{X}^{\text{H}} \mathbf{y}\|_2^2]. \quad (17)$$

Due to the possibility to apply fast Fourier transform (FFT) for the two-dimensional circular convolution and the pilot matrix, the overall complexity of the estimator is only $\mathcal{O}(N_{\text{tx}} N_{\text{rx}} \log(N_{\text{rx}} N_{\text{tx}}))$.

V. BASELINE ALGORITHMS

In the QuaDRiGa software, the channel covariance matrix for each channel realization is not available. Therefore, we do not have perfect knowledge of the second-order channel statistics in order to evaluate the optimal linear minimum mean square error (LMMSE) estimator. However, to have a reasonable baseline, we evaluate the LMMSE with the sampled global covariance matrix $\hat{\mathbf{C}}_{\text{glob}}$, cf. (3). The estimate then reads as

$$\hat{\mathbf{h}}_{\text{LMMSE}} = \hat{\mathbf{C}}_{\text{glob}} \mathbf{X}^{\text{H}} (\mathbf{X} \hat{\mathbf{C}}_{\text{glob}} \mathbf{X}^{\text{H}} + \sigma^2 \mathbf{I}_{N_{\text{rx}} N_{\text{p}}})^{-1} \mathbf{y}. \quad (18)$$

Note that this clearly is a suboptimal approach as the global covariance matrix is different from the conditional covariance matrix \mathbf{C}_{δ} which takes account of the prior δ . To further evaluate the UL-DL conjecture described above, we evaluate the LMMSE for both, the sampled global covariance matrix of UL and DL channels.

In massive MIMO systems, the channel covariance matrices have a low numerical rank [21], and therefore, the channel vector \mathbf{h} can be approximated by a sparse vector \mathbf{t} for a given dictionary \mathbf{D} , i.e., $\mathbf{h} \approx \mathbf{D} \mathbf{t}$. A reasonable choice for the dictionary is $\mathbf{D} = \mathbf{D}_{\text{rx}} \otimes \mathbf{D}_{\text{tx}}$, where \mathbf{D}_{rx} and \mathbf{D}_{tx} are oversampled DFT matrices [22]. This choice is motivated by the fact that the DFT matrix maps to the sparse angular domain in case of a ULA. The vector \mathbf{t} can then be found by solving a sparse approximation problem, for which the orthogonal matching pursuit (OMP) algorithm is suitable [23]. As the sparsity order is unknown, we use a genie-aided upper bound in our simulations, which decides about the sparsity level with the given exact channel realization.

Another low-complexity CE algorithm is maximum likelihood (ML) estimation of the structured covariance matrix [24], [25]. The estimate with the block-circular assumption for the covariance matrix is

$$\hat{\mathbf{h}} = \mathbf{Q}^{\text{H}} \text{diag}(\mathbf{c}_{\delta}^{\text{ML}}) (\mathbf{N} \mathbf{U}^{-1} \text{diag}(\mathbf{c}_{\delta}^{\text{ML}}) + \sigma^2 \mathbf{I}_{S\text{U}})^{-1} \tilde{\mathbf{Q}} \mathbf{y}$$

with $\tilde{\mathbf{Q}} = \mathbf{Q} \mathbf{X}^{\text{H}}$. The eigenvalues of \mathbf{C}_{δ} are estimated as $\mathbf{c}_{\delta}^{\text{ML}} = [\mathbf{s} - \sigma^2 \mathbf{1}]_+$, where $\mathbf{s} = |\mathbf{Q} \mathbf{X}^{\text{H}} \mathbf{y}|^2$ and the i th element of $[\mathbf{x}]_+$ is $\max(x_i, 0)$, cf. [15]. We further show the least squares (LS) solution which minimizes the ℓ_2 norm $\|\mathbf{y} - \mathbf{X} \mathbf{h}\|_2$ [26].

VI. SIMULATION RESULTS

We depict numerical results where we simulated the proposed learning strategy described in Subsection I-A with data that is generated with the QuaDRiGa software, cf. Section III.

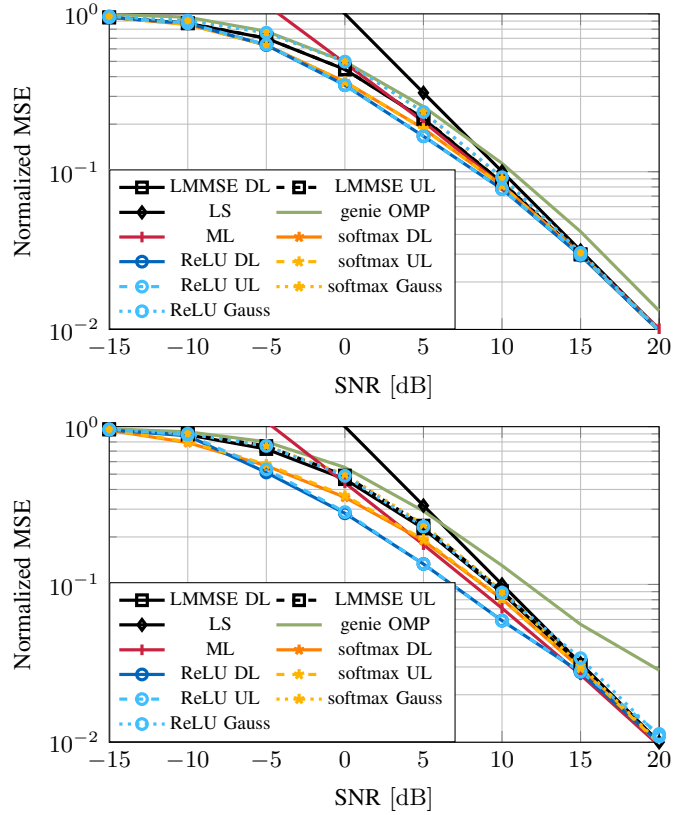


Fig. 2: Comparison of CNN estimator trained on UL or DL data with baseline approaches for mixed NLOS/LOS scenario. Top: $(N_{\text{tx}}, N_{\text{rx}}, N_{\text{p}}) = (8, 4, 8)$, bottom: $(N_{\text{tx}}, N_{\text{rx}}, N_{\text{p}}) = (64, 4, 64)$.

We evaluate the described CNN estimator from Section IV which is trained solely on UL data and has never seen DL channels in the training phase for two different activation functions: ReLU and softmax. We refer to these results as "ReLU UL" and "softmax UL", respectively. Note that the evaluation data always stem from actual DL channels. For direct comparison, we depict the same CNN estimator which is trained on DL channels directly, referred to as "ReLU DL" and "softmax DL", respectively. For verification that the proposed CNN estimator indeed learns structural features of the chosen scenario, we show results where the input channels for the CNN in the training phase are purely i.i.d. Gaussian channels, without any structural properties that occur in the UMa scenario. We refer to this results as "ReLU Gauss" and "softmax Gauss", respectively. Lastly, we evaluate the LMMSE estimator which uses the sampled global covariance matrix from (3), sampled from DL channels ("LMMSE DL") and UL channels ("LMMSE UL"), respectively.

In Fig. 2, we compare the different estimators for different SNRs ranging from -15 dB to 20 dB for a 4×8 (top) and 4×64 (bottom) MIMO setup. First of all, one can observe that the CNN estimator performs equally well when being trained on either data which stem from the DL or UL. This can be observed for both setups and therefore validates the

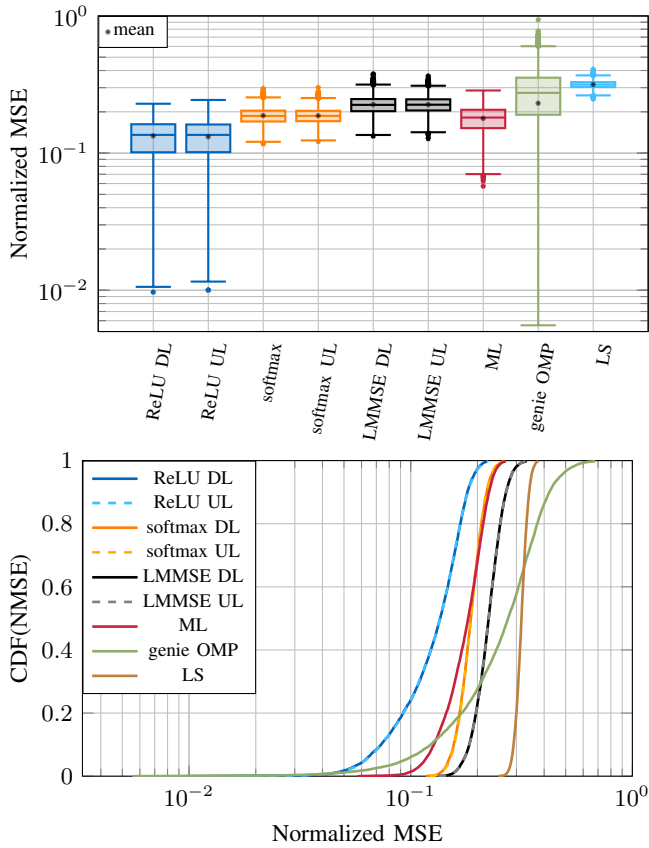


Fig. 3: Boxplot (top) and CDF curves (bottom) for mixed NLOS/LOS scenario with $(N_{\text{tx}}, N_{\text{rx}}, N_P) = (64, 4, 64)$ for SNR = 5dB.

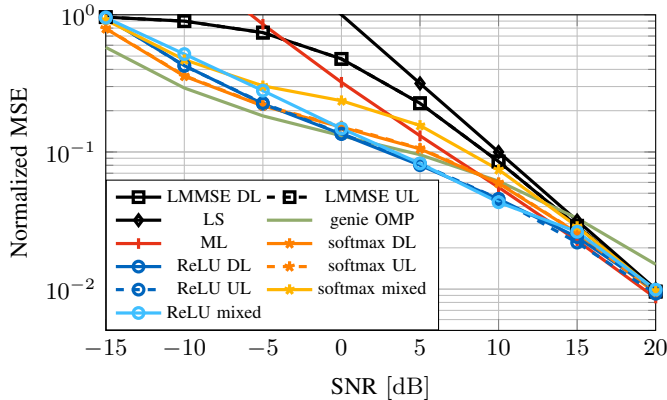


Fig. 4: Comparison of CNN estimator trained on UL or DL data with baseline approaches evaluated on LOS channels for $(N_{\text{tx}}, N_{\text{rx}}, N_P) = (64, 4, 64)$.

UL-DL conjecture stated in [11] and [12]. One can further observe a performance gap to the CNN estimator trained on i.i.d. Gaussian channels. This indicates that the CNN estimator is able to adapt to the scenario by inferring structural properties of the data that is provided in the training phase. Since the UL and DL data stem from the same scenario, it seems that common features are shared between both domains.

Furthermore, the performance gap as compared to training with Gaussian data increases for the higher-dimensional setup (bottom), which may be due to more structure within the data in larger setups, e.g., due to antenna correlations.

The same argumentation holds for the comparison with the LMMSE, either based on UL or DL channels. Due to the global sampling of the covariance matrix, there is no structural information that is exploited by the estimator as this is averaged out (the h_i in (3) are found all over the cell). If we further compare the CNN estimator with the baseline approaches LS, ML, and genie OMP, the superiority of the learning-based approach becomes clear. Especially the CS-based approach OMP is not able to compete with the proposed learning-based approach. This may be caused by the difficulty of the UMa scenario, in which many channels are NLOS channels with many subpaths, which again are constructed by the superposition of many micropaths. In such scenarios, the underlying sparsity may either not be given, or it can not be exploited by the OMP algorithm with the given dictionary.

After we have seen that the CNN estimator performs equally well on average, independent of whether the training data stems from UL or DL, we now want to investigate this more precisely by looking at the naturally occurring variations of the estimation performance over many samples in terms of MSE for a fixed SNR of 5dB. This variation is caused by the difference of the channel samples, e.g., by being LOS or NLOS channels, and therefore being easier or harder to estimate in general. In Fig. 3, these variations are evaluated in form of a boxplot (top) and in form of their cumulative distribution functions (CDFs) (bottom). For the boxplot, the lower and upper box edges indicate the first and third quartile, respectively, and the middle line the median (50th percentile). For convenience, we also show the mean values (dots). From the lower (upper) box edges, a distance of 1.5 times the interquartile range (IQR) is measured where a whisker is drawn up to the lowest (largest) observed point from the dataset that falls within this distance. All other observed points are plotted as outliers.

It can be observed that the boxplots for the estimators based on UL and the ones based on DL data are very similar and that their CDFs are lying on top of each other. This means that the estimators are not only performing equally well on average, it can be expected that the estimators also show very similar performance on instantaneous channel realizations. Here, it is important to keep in mind that the test set on which the plots are based are the same and stem from DL channels.

We can see further that the CNN estimator with ReLU not only shows the best performance on average, but its upper whisker is also bounded tightly at the lowest MSE compared to the baseline algorithms. The performance of the genie OMP, however, strongly depends on the instantaneous channel realizations and therefore shows a huge variation in terms of MSE. When looking at the CDF, the genie OMP can achieve very good performance with low probability, but fails to achieve a certain error bound with high probability in such a difficult scenario.

In addition to the already shown scenario with mixed NLOS and LOS channels, we now evaluate a UMa scenario with pure LOS channels. The LOS channels have a single dominant subpath and are therefore more easily sparsely representable. In addition to the approaches we already discussed before, we depict the CNN estimator which is trained on the dataset from before with mixed NLOS and LOS channels, but is evaluated on the pure LOS, referred to as "ReLU mixed" and "softmax mixed". It can be seen that especially the genie OMP approach benefits from the pure LOS scenario, especially for low to medium SNR values. However, the learning-based approaches outperform the CS approach also in this scenario for higher SNR values. Besides the observation that the UL-DL conjecture also holds for the LOS scenario, it conveys that the CNN approach with ReLU activation trained on mixed NLOS and LOS channels almost achieves the same performance as the one that is trained purely on LOS channels. This makes the great generalization ability of the learning-based CNN approach visible. The LS and LMMSE approach are not able to exploit the structural simplifications of the scenario and therefore show no gain compared to the mixed NLOS and LOS scenario.

VII. CONCLUSION

In this work, we proposed a novel signaling approach for centralized learning of the distributed DL channel estimators in FDD systems. This is based on the observation that, regardless of the difference of the instantaneous UL and DL channels, the UL dataset can be used for training the DL channel estimator due to the similar distributions of UL and DL channels. This again illustrates nicely the fact that neural networks are not dependent on specific data samples, but rather learn the underlying distribution of the provided dataset.

We outlined an approach where the CNN of a low-complexity MIMO channel estimator is trained at the BS and just the network parameters are offloaded to the MT. This procedure immediately resolves the problems of data generation, storage, and (re-)training of the CNN at the MT which is closely associated with power-efficiency constraints. Although the signaling strategy is presented for the recently proposed MIMO CNN estimator, it may also be useful for different data-aided approaches in DL CE. We presented numerical results which validate the reasonability of the approach and further show that the learning-based approach outperforms state-of-the-art approaches due to the possibility of incorporating knowledge of the scenario that is available from the provided dataset.

REFERENCES

- [1] T. L. Marzetta, "Noncooperative Cellular Wireless with Unlimited Numbers of Base Station Antennas," *IEEE Trans. Wireless Commun.*, vol. 9, no. 11, pp. 3590–3600, 2010.
- [2] E. Björnson, J. Hoydis, M. Kountouris, and M. Debbah, "Massive MIMO Systems With Non-Ideal Hardware: Energy Efficiency, Estimation, and Capacity Limits," *IEEE Trans. Inf. Theory*, vol. 60, no. 11, pp. 7112–7139, 2014.
- [3] Y. Xu, G. Yue, and S. Mao, "User Grouping for Massive MIMO in FDD Systems: New Design Methods and Analysis," *IEEE Access*, vol. 2, pp. 947–959, 2014.
- [4] X. Rao and V. K. N. Lau, "Distributed Compressive CSIT Estimation and Feedback for FDD Multi-User Massive MIMO Systems," *IEEE Trans. Signal Process.*, vol. 62, no. 12, pp. 3261–3271, Jun. 2014.
- [5] Z. Gao, L. Dai, Z. Wang, and S. Chen, "Spatially Common Sparsity Based Adaptive Channel Estimation and Feedback for FDD Massive MIMO," *IEEE Trans. Signal Process.*, vol. 63, no. 23, pp. 6169–6183, 2015.
- [6] Z. Gao, L. Dai, W. Dai, B. Shim, and Z. Wang, "Structured Compressive Sensing-Based Spatio-Temporal Joint Channel Estimation for FDD Massive MIMO," *IEEE Trans. Commun.*, vol. 64, no. 2, pp. 601–617, 2016.
- [7] Y. Han, J. Lee, and D. J. Love, "Compressed Sensing-Aided Downlink Channel Training for FDD Massive MIMO Systems," *IEEE Trans. Commun.*, vol. 65, no. 7, pp. 2852–2862, 2017.
- [8] X. Ma and Z. Gao, "Data-Driven Deep Learning to Design Pilot and Channel Estimator for Massive MIMO," *IEEE Trans. Veh. Technol.*, vol. 69, no. 5, pp. 5677–5682, 2020.
- [9] M. B. Mashhadi and D. Gündüz, "Pruning the Pilots: Deep Learning-Based Pilot Design and Channel Estimation for MIMO-OFDM Systems," *IEEE Trans. Wireless Commun.*, 2021.
- [10] J. Guo, C.-K. Wen, and S. Jin, "CANet: Uplink-aided Downlink Channel Acquisition in FDD Massive MIMO using Deep Learning," 2021, <https://arxiv.org/abs/2101.04377>.
- [11] W. Utschick, V. Rizzello, M. Joham, Z. Ma, and L. Piazzi, "Learning the CSI Recovery in FDD Systems," 2021, <https://arxiv.org/abs/2104.01322>.
- [12] V. Rizzello and W. Utschick, "Learning the CSI Denoising and Feedback Without Supervision," 2021, <https://arxiv.org/abs/2104.05002>.
- [13] N. Turan, M. Koller, S. Bazzi, W. Xu, and W. Utschick, "Unsupervised Learning of Adaptive Codebooks for Deep Feedback Encoding in FDD Systems," 2021, <https://arxiv.org/abs/2105.09125>.
- [14] B. Fesl, N. Turan, M. Koller, and W. Utschick, "A Low-Complexity MIMO Channel Estimator with Implicit Structure of a Convolutional Neural Network," 2021, <https://arxiv.org/abs/2104.12667>.
- [15] D. Neumann, T. Wiese, and W. Utschick, "Learning the MMSE Channel Estimator," *IEEE Trans. Signal Process.*, vol. 66, no. 11, pp. 2905–2917, 2018.
- [16] M. Biguesh and A. Gershman, "Training-based MIMO Channel Estimation: A Study of Estimator Tradeoffs and Optimal Training Signals," *IEEE Trans. Signal Process.*, vol. 54, no. 3, pp. 884–893, Mar. 2006.
- [17] S. Jaeckel, L. Raschkowski, K. Börner, and L. Thiele, "Quadriga: A 3-d multi-cell channel model with time evolution for enabling virtual field trials," *IEEE Trans. Antennas Propag.*, vol. 62, no. 6, pp. 3242–3256, 2014.
- [18] S. Jaeckel, L. Raschkowski, K. Börner, L. Thiele, F. Burkhardt, and E. Eberlein, "Quadriga: Quasi deterministic radio channel generator, user manual and documentation," Fraunhofer Heinrich Hertz Institute, Tech. Rep., v2.2.0, 2019.
- [19] 3GPP, "Study on channel model for frequencies from 0.5 to 100 GHz," 3rd Generation Partnership Project (3GPP), TR 38.901 V16.1.0, 2019.
- [20] M. Kurras, S. Dai, S. Jaeckel, and L. Thiele, "Evaluation of the spatial consistency feature in the 3gpp geometry-based stochastic channel model," in *2019 IEEE Wireless Commun. and Netw. Conf. (WCNC)*, 2019, pp. 1–6.
- [21] T. Wiese, L. Weiland, and W. Utschick, "Low-Rank Approximations for Spatial Channel Models," in *Proc. 19th Int. ITG Workshop Smart Antennas*, 2016.
- [22] A. Alkhateeb, G. Leus, and R. W. Heath, "Compressed Sensing based Multi-User Millimeter Wave Systems: How many Measurements are Needed?" in *IEEE Int. Conf. Acoust. Speech Signal Process.*, 2015, pp. 2909–2913.
- [23] M. Gharavi-Alkhansari and T. S. Huang, "A Fast Orthogonal Matching Pursuit Algorithm," in *Proc. IEEE Int. Conf. Acoust. Speech Signal Process.*, vol. 3, May 1998, pp. 1389–1392.
- [24] D. Neumann, M. Joham, L. Weiland, and W. Utschick, "Low-Complexity Computation of LMMSE Channel Estimates in Massive MIMO," in *Proc. 19th Int. ITG Workshop Smart Antennas*, 2015.
- [25] J. P. Burg, D. G. Luenberger, and D. L. Wenger, "Estimation of Structured Covariance Matrices," *Proc. IEEE*, vol. 70, no. 9, pp. 963–974, 1982.
- [26] M. Biguesh and A. B. Gershman, "Training-Based MIMO Channel Estimation: A Study of Estimator Tradeoffs and Optimal Training Signals," *IEEE Trans. Signal Process.*, vol. 54, no. 3, pp. 884–893, 2006.